Talanta 265 (2023) 124814

Contents lists available at ScienceDirect

Talanta

journal homepage: www.elsevier.com/locate/talanta

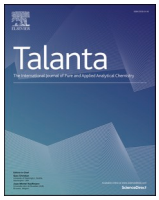

Single-cell microfluidics enabled dynamic evaluation of drug combinations on antibiotic resistance bacteria

Xiaobo Li [a,b,1], Yanqing Song [b,1], Xiuzhao Chen [a], Jianan Yin [a], Ping Wang [c], He Huang [a,*], Huabing Yin [b]

[a] School of Chemical Engineering and Technology, Key Laboratory of Systems Bioengineering (Ministry of Education), Frontiers Science Center for Synthetic Biology, Tianjin University, Tianjin, 300072, China
[b] James Watt School of Engineering, University of Glasgow, G12 8LT, UK
[c] Tianjin Modern Innovative TCM Technology Co. Ltd., 300392, China

ARTICLE INFO

Handling Editor: Qun Fang

Keywords:
Acinetobacter baumannii
Antibiotic resistance
Microfluidics
Single-cell analysis
Berberine hydrochloride
Combination treatment

ABSTRACT

The rapid spread of antibiotic resistance has become a significant threat to global health, yet the development of new antibiotics is outpaced by emerging new resistance. To treat multidrug-resistant bacteria and prolong the lifetime of existing antibiotics, a productive strategy is to use combinations of antibiotics and/or adjuvants. However, evaluating drug combinations is primarily based on end-point checkerboard measurements, which provide limited information to study the mechanism of action and the discrepancies in the clinical outcomes. Here, single-cell microfluidics is used for rapid evaluation of the efficacy and mode of action of antibiotic combinations within 3 h. Focusing on multidrug-resistant *Acinetobacter baumannii,* the combination between berberine hydrochloride (BBH, as an adjuvant) and carbapenems (meropenem, MEM) or β-lactam antibiotic is evaluated. Real-time tracking of individual cells to programmable delivered antibiotics reveals multiple phenotypes (i.e., susceptible, resistant, and persistent cells) with fidelity. Our study discovers that BBH facilitates the accumulation of antibiotics within cells, indicating synergistic effects (FICI = 0.5). For example, the combination of 256 mg/L BBH and 16 mg/L MEM has a similar killing effect (i.e., the inhibition rates >90%) as the MIC of MEM (64 mg/L). Importantly, the synergistic effect of a combination can diminish if the bacteria are pre-stressed with any single drug. Such information is vital for understanding the underlying mechanisms of combinational treatments. Overall, our platform provides a promising approach to evaluate the dynamic and heterogenous response of a bacterial population to antibiotics, which will facilitate new drug discovery and reduce emerging antibiotic resistance.

1. Introduction

The rapid spread of antibiotic resistance has become a significant crisis in the 21st century. Not only have bacteria become resistant to existing antibiotics, but new resistance mechanisms are constantly emerging, significantly outpacing new antibiotics' development. Recent surveys have shown that less than ten antibacterial agents have been approved by FDA since 2017, none of which is against Gram-negative strains [1]. For those in the preclinical pipeline, substantial translational hurdles have yet to be overcome [2]. These hurdles would only lead to an escalated crisis in the post-antibiotic era without immediate action [3].

Many multidrug-resistant pathogens are sensitive to few or no antibiotics. A typical example can be seen in multidrug-resistant *Acinetobacter baumannii* (MDR *A. baumannii*), which causes most hospital-acquired infections and high mortality rates in intensive care units [4]. Currently, few options exist to treat MDR *A. baumannii*-related infections [5]. Carbapenems used to be "last-line" antibiotics until recently when carbapenem-resistant *A. baumannii* escalated globally and is on the top list of the WHO priority pathogens [6]. In the absence of new-class antibiotics to treat these multidrug-resistant Gram-negative infections, combination therapy has been a vital option to treat severe cases, especially when monotherapy fails [7].

Combinations of existing antibiotics or antibiotics with non-

* Corresponding author.
E-mail addresses: huang@tju.edu.cn (H. Huang), huabing.yin@glasgow.ac.uk (H. Yin).
[1] These authors contributed equally to this work.

https://doi.org/10.1016/j.talanta.2023.124814
Received 12 April 2023; Received in revised form 8 June 2023; Accepted 11 June 2023
Available online 16 June 2023
0039-9140/© 2023 The Authors. Published by Elsevier B.V. This is an open access article under the CC BY license (http://creativecommons.org/licenses/by/4.0/).

antibiotic adjuvants have already been used in clinics to treat severe infections [8,9]. Some defined formulations, such as the streptomycin/penicillin combination, have been verified as a congruous synergism to treat enterococcal infections [8]. Antibiotic combinations are usually evaluated with the checkerboard method using static antibiotic concentrations. However, many in vitro studies are conflicting, and despite some combinations showing enhanced efficacy in vitro, their clinical outcomes are often contradictory [7,10]. These discrepancies are widely recognized and reflect the complexity of the interactions between multiple compounds regarding their inhibition or killing mechanisms on bacteria [11].

One fact contributing to the complexity is the heterogeneity of individual bacterial cells in a population. These individual differences play an important role in bacteria surviving lethal antibiotic stress [12]. Different phenotypes, such as resistant cells, persistent cells, and viable but non-dividing cells, have all been observed in bacteria isolates, which can contribute to antibiotic-treatment failures and the recurrence of infections [13–15]. The heterogeneous phenotypes, albeit in small numbers in a population, can be triggered by many factors [14,16]. In addition, there are links between antibiotic-resistant cells and other phenotypes, such as persistent cells [17,18]. However, traditional in vitro screening of antibiotic combinations is based on an end-point measurement of the minimum inhibitory concentration of a bulk culture. It thus can't reveal these keys, hidden heterogeneous responses.

The advancement of microfluidic technologies has fuelled the rapid development of pathophysiological studies and drug discovery [19,20], especially, single-cell technology-based research, which enables in situ observation of individual cells under well-controlled conditions [21–24]. Microfluidic devices, such as mother machine [25], agarose microfluidic channels [26] and chemostatic devices [27] have been used to immobilize cells on-chip to allow real-time tracking of individual cells under imposed stresses. Many phenomena, such as antibiotic-induced opportunistic persistence [28], and the evolution of microorganisms under antibiotic treatments [29] have been discovered, which significantly accelerate our understanding of factors that contribute to the failure of antibiotic treatments.

Here, we demonstrate single-cell microfluidics as a powerful platform for investigating the effectiveness and mechanisms of antibiotic combinations. We focus on evaluating the potential of carbapenems antibiotics with berberine hydrochloride (BBH, an extract from plants) as an adjuvant to treat MDR *A. baumannii*. Recently, it was found that BBH can re-sensitize MDR *A. baumannii* to some broad-spectrum β-lactam antibiotics that are barely effective due to bacterial resistance [30]. By in situ monitoring individual cells over time, we can quantitatively measure their growth characteristics (e.g., growth rate and lag time) and the heterogeneity of the population. This, coupled with the programmable delivery of different drug treatments, allowed us to identify different phenotypes (i.e., susceptible, dormant, resistant, and persistent cells). Importantly, the time-course delivery of the combination compounds provides vital information to understand interactions between the compounds and the mode of action. We show that single-cell approaches can provide rapid, rich information to guide bulk or in vivo testing and enhance our ability to evaluate and predict the efficacy of new combination therapy.

2. Materials and methods

2.1. Microfluidic platform

The microfluidic platform was fabricated as described previously [31]. In brief, a PDMS replica was made against a silicon mould, and then it was bonded to a clean coverslip through oxygen plasma treatment. The platform consists of two parallel channels (50 μm width × 10 μm height) and eight identical microchambers (200 μm length × 80 μm width × 0.74 μm height). A lower height region (about 0.4 μm) served as a barrier to block cells in the chamber during the cell loading process.

2.2. Bacterial strains and antimicrobial agents

A. baumannii strain MDR-TJ was isolated from a patient's sputum at the Second Hospital of Tianjin Medical University, China [32], and its resistance profile showed in Table S1. The strain was stored in LB broth with 25% glycerol at −80 °C and was streaked to form a single colony to ensure optimal growth and purity before testing. Berberine hydrochloride, sulbactam, meropenem, and mecillinam were dissolved in sterilized deionized water at a final concentration of 2048 mg/L and stocked at −20 °C.

2.3. MIC determination and synergy assays

A microdilution broth method was used to determine the MICs (Minimum Inhibitory Concentrations) recommended by the document M100 of the CLSI [33]. The checkerboard assay was used to determine in vitro synergistic activity of antibiotic combinations [34].

2.4. Cell culture and inhibitory tests on chip

MDR-TJ strain was cultured in cation-adjusted Mueller Hinton broth (CAMHB) at 37 °C overnight and then re-cultured with a dilution of 1% in the same fresh medium to reach an OD_{600nm} of about 0.6–0.8. Cells were centrifuged, washed twice with PBS, and then diluted with PBS to an OD_{600nm} of about 0.02 as the cell loading solution. The cell solution was delivered through the loading channel at a speed of 2 μL/min whilst the medium was delivered through the other channel at 0.15 μL/min to trap cells in the microchambers. After that, only the medium was delivered to both channels and kept at 0.15 μL/min. All on-chip cultures were performed at 37 °C in a commercial thermos plate (TPi-SQX, Tokai Hit Co., Ltd., Japan). A more homogeneous population was found at 37 °C compared to that at room temperature (~25 °C) (See Fig. S1). For inhibitory tests, the antimicrobials of designed concentrations were added to the CAMHB medium, and the CAMHB medium only was used as the control. For kinetic studies, the CAMHB medium was used to replace the drug-containing solutions whenever needed.

2.5. Live/dead cell staining

LIVE/DEAD BacLight Bacterial Viability Kit (L13152, Invitrogen) was used for characterising live and dead cells at the end of tests. The flow rate of the staining solution (30 μM of propidium iodide and 6 μM SYTO 9 in PBS) was maintained at 0.15 μL/min. Fluorescence imaging was conducted after ~1.0 h of staining. SYTO 9 (green) was detected using 455–495 nm (excitation)/505–555 nm (emission) and propidium iodide (red) using 533–558 nm (excitation)/570–640 nm (emission), respectively.

2.6. Image acquisition

A fluorescence inverted microscope (Zeiss Axio Observer 7) equipped with a 40 × /0.6 objective lens or an inverted fluorescence microscope (Olympus I×83) equipped with a 60 × /0.70 objective lens was used to record bright field and fluorescence images. Time-lapse images were acquired at an interval of 20 min or 10 min throughout the experiments.

2.7. Calculation of the growth parameters μ and λ

All images were processed with Image J to calculate the specific growth rates (μ) and lag time (λ) as previously described (also see Fig. S2) [31].

2.8. TDtest essay

The TDtest assay was performed to verify whether MDR-TJ showed bacterial tolerance or persistence under the meropenem (MEM)

treatment [35]. The procedure contains three steps: 1). 100 μL of bacterial suspension ($OD_{600nm} = 0.2$) was spread onto an MHA plate before adding 60 μg of MEM to the centre of this plate to form an inhibition zone. 2). 2 mg of glucose was added to the centre of the inhibition zone for identifying tolerant or persistent cell growth. 3). The tolerant or persistent colony was picked up for inhibition tests following the procedure in step 1). Tolerance or persistence was confirmed if they shared the identical inhibition zone with their parental strain.

2.9. Statistical analysis

For each condition, at least two to three independent experiments were conducted, and 60–100 single colonies were randomly selected. All results were shown as the mean ± standard deviation. Statistical analysis was carried out with the unpaired one-way analysis of variance (ANOVA) by GraphPad Prism 8 software system. Statistical significance was determined when the P value < 0.05.

3. Results

3.1. Multi-step assay on-chip and real-time monitoring of individual cells

A multi-layered microfluidic device was fabricated as described before (Fig. 1a) [31]. Cells were trapped in the middle chambers to form a monolayer cell culture, facilitating in situ imaging. Medium, with or without antibiotics, was delivered continuously from the side channels. This continuous flow culture removed metabolic waste and maintained the nutrients, akin to a chemostat culture. The flow rates in both side channels can be easily controlled to achieve the required operations, namely 1) cell trapping, 2) rapid exchanging of reagents, 3) removing overgrowing cells from the chamber, and 4) collecting targeted cells off-chip. These capabilities allow real-time observation of the same cells under a series of antibiotic treatment regimens (e.g., single drug, combined drug, in sequential drug treatments), revealing diverse phenomena of dynamical responses of individual cells. Importantly, successive assays can be applied to identify rare subpopulations of resistant or persistent cells with fidelity and retrieve them off-chip for further studies. This function offers unique advantages in linking single-cell studies with conventional population methods compared with previous systems [15].

MDR *A. baumannii* cells are normally short, rod-shaped and present as a pair of two connected cells (Fig. 1b). Typical time-lapse images showed that most single colonies started from a single pair that was also divided as a pair (Fig. 1b, indicated by red stars) as if they were one entity. Since a pair behaved as one entity, the colonies derived from one pair can be considered "single-cell" colonies. With the culture medium alone, most cells grew, but a few cells did not show any changes over the whole duration of on-chip testing (i.e., 2 h), which are termed as "dormant cells" (Fig. 1b, indicated by red arrows).

Colonies originating from these growing individual cells/single pairs were analysed from time-lapse images to derive their specific growth rates (μ, h^{-1}) and lag times (λ, h) (i.e., the delay time in the growth phase when bacteria adapt to new environments) (Fig. S2) [23]. With these rich individual data, we can easily derive the average values of the population and the heterogeneity of the population from the correlated individual μ−λ distributions [31]. Furthermore, the duration of the lag phase can indicate how bacteria cells resist antibiotic stress, and often extended lag time offers bacteria survival advantages and promotes regrowth upon the removal of antibiotics [36,37].

It was found that the average growth rates μ of the population from the single-cell on-chip assay ($1.61 \pm 0.17\ h^{-1}$) matched well with that of conventional broth culture ($1.44\ h^{-1} \pm 0.24\ h^{-1}$) at 37 °C (Table S2). In addition, most of the cells had a short lag time for on-chip culture (~0.1 h), indicating the excellent ability of MDR *A. baumannii* to adapt to new

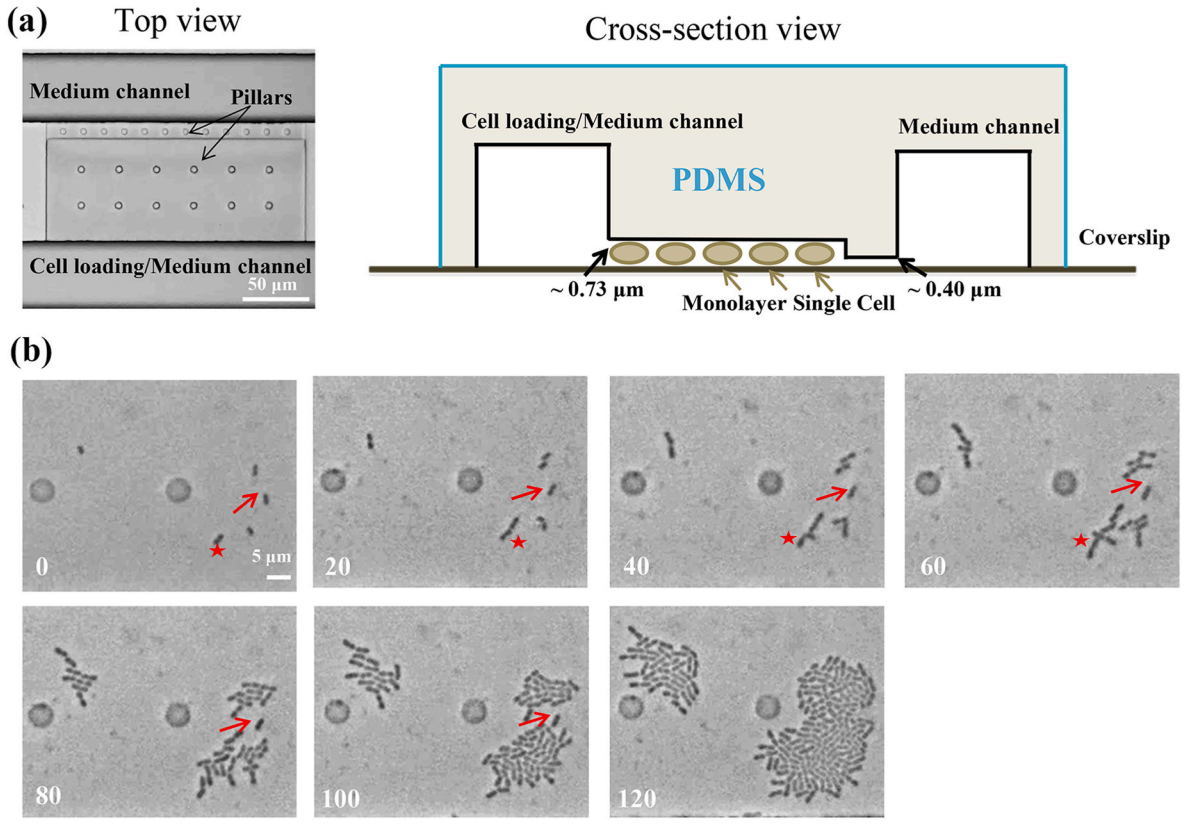

Fig. 1. (a) The microfluidic device. The side channels were used to deliver cells and medium. A monolayer of cells was trapped in the middle microchamber. (b) Typical time-lapse optical images of the MDR *A. baumannii* in microchambers.

environments.

3.2. Characterize the dynamic inhibition processes by each compound

To understand the action of a synergistic combination in treating multidrug-resistant bacteria, an in-depth evaluation of how each compound inhibits the strain is indispensable. Using the microfluidic device, we first tracked the real-time response of the MDR-TJ strain treated by either BBH or MEM alone, as detailed below. The morphological variations and growth characteristics of individual cells under a range of concentrations reveal invaluable information about the means deployed by the resistant strain to battle the antibiotics.

BBH has weak antibacterial activity against MDR *A. baumannii* with a MIC value of 1024 mg/L (Table S3). The on-chip study showed that most cells kept dividing and hardly changed their morphology, even at 800 mg/L BBH (Fig. 2a). For these dividing cells, the average growth rate was slightly reduced to 1.35 h^{-1} with 256 mg/L BBH and to 1.35 h^{-1} with 800 mg/L BBH in comparison with the control without BBH (i.e., 1.61 h^{-1}) (Fig. 2d). However, there were no significant effects on the cells' lag time (Fig. 2e). Interestingly, it was found that the percentage of dormant cells increased to 6.79% with 256 mg/L BBH and to 25.4% with 800 mg/L BBH, compared to 1.95% under control (Table S4). Although the dormant cells did not divide, live/dead assays revealed that some are viable (Fig. 2a, indicated by a white circle). Dormant cells have low metabolic activities, which has been an important mechanism for bacteria to tolerate antibiotic stress [15]. These results suggested that the MDR *A. baumannii* strain contains a range of heterogeneous phenotypes, and BBH could reduce the metabolic activities of cells.

Meropenem (MEM) is a broad-spectrum carbapenem antibiotic and the MDR-TJ strain is resistant to MEM based on the MIC of MEM (i.e., 64 mg/L) (Table S3). MEM treatments induced obvious morphological changes in cells, which also depended on both time and MEM concentrations (Fig. 2b). At a lower concentration (i.e., 16 mg/L MEM), most individual cells began to swell after 80 min. However, most of the pairs kept dividing in the new dumbbell shape (indicated by the red arrows in Fig. 2b). Like the effect of 800 mg/L BBH, no significant difference in lag time was observed, and the average growth rate reduced to 1.36 h^{-1} (i.e., 84.5% of the control, $P < 0.0001$) (Fig. 2d). The distribution of individual cell growth rates widened significantly. Since MEM mainly targets penicillin-binding proteins (PBPs) - the essential enzymes for the synthesis of the bacterial cell wall [38], the morphological transformation directly reflects the degree of growth inhibition by the MEM stress, which is characterized by substantial heterogeneity in cell responses at the sub-MIC concentration of 16 mg/L.

At the MIC of MEM (i.e., 64 mg/L), the swelling of some cells occurred much earlier (~40 min) in comparison with MEM at 16 mg/L. For the initially growing cells, their growth rates started to decline after 20 min (i.e., negative gradient) (Fig. 2c), indicating the disintegration of cells. Many cells remained unchanged throughout the 2-h treatment and were confirmed dead with PI staining (Fig. 2b). These unchanged cells were also been lysed in the later stage (indicated by the red circle in Fig. 2b). This suggests that high MEM concentrations accelerated the

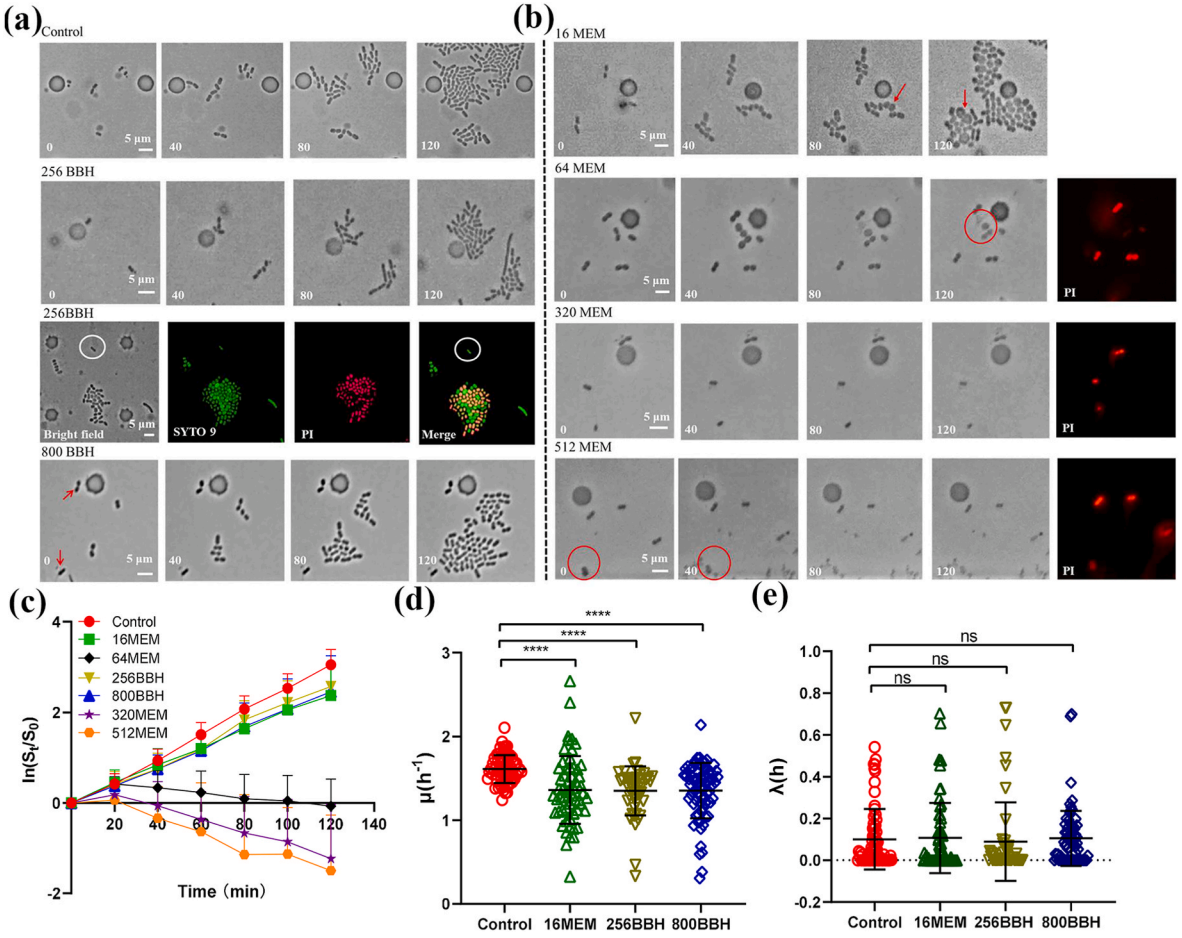

Fig. 2. Time-lapse images of MDR *A. baumannii* under treatments by (a) BBH or (b) MEM alone at different concentrations (unit, mg/L) for 120 min. Live cell staining (SYTO9, green colour) and dead cell staining (propidium iodide, red colour) were performed to verify cell status. Images for 800 mg/L BBH are similar to 256 mg/L BBH. No live cells were observed for MEM>64 mg/L. The growth curves (c), the specific growth rate (d), and the lag time (e) of MDR *A. baumannii* at different drug concentrations. BBH: berberine hydrochloride; MEM: meropenem. (****$p < 0.0001$, one-way ANOVA with Tukey's post hoc comparison).

inactivation of PBPs, leading to rapid cell death and, subsequently cell lysis. Similar results were observed at the higher MEM concentrations of 320 mg/L and 512 mg/L (i.e., 5x and 8x of the MIC value) with steeper negative gradients of colony growth after 20 min (Fig. 2c), indicating faster disintegration of dead cells. These results demonstrated that the higher concentration, the faster the inhibition/killing action of MEM.

It is worth noting that many cells did not show any changes at ≥ MIC concentrations. Although most were PI stained as dead cells, few cells may survive under these lethal treatments. Previous work showed such cells, either as persistent cells or tolerate cells, were commonly found in multi-drug resistance bacteria, and contributed to the failure of antibiotic treatments [39,40]. To examine their existence, after 5 h of treatment with 512 mg/L MEM, a fresh medium was reintroduced to culture cells (Fig. 3a). It was found that a few cells resumed their growth after a long lag time (about 9.5 h) with a growth rate of 1.91 h^{-1} (Fig. S3), reaching similar initial growth rates to that without antibiotic treatment. However, these cells are rare in the population (<0.04%, Table S5). Notably, via changing pressure in both side channels, we were able to release these regrowing cells from the chip and collect them for off-chip culture and additional assays. It was found that their MIC values against MEM (64 mg/L) were the same as the original cells (Table S5), which resembled previously reported drug-induced persistent cells [14].

To corroborate our findings from the single-cell study, we further carried out the population-based TDtest essay as reported [35]. After adding glucose to the centre of the inhibition zone, several colonies formed in the inhibition zone (Fig. 3b), illustrating the existence of the tolerant/persistent cells in the population. These results proved that high MEM concentration could induce persistent cells in MDR *A. baumannii,* suggesting the importance of using suitable antibiotic dosages in clinical treatments.

3.3. Phenotypical changes provide insights into the mode of action of BBH/MEM combination

Next, we employed the single-cell platform to investigate the response of MDR *A. baumannii* under the treatment of BBH/MEM combinations. Via conventional checkboard assays, we found that the total fractional inhibitory concentration index (FICI) of BBH/MEM combinations is 0.5 (Table S3), which indicates a synergistic effect [34]. The MIC concentration for the BBH/MEM combination is 256 mg/L BBH with 16 mg/L MEM, which reduces the MEM dose to one-quarter of its MIC when used alone. To evaluate whether the synergy could be applied to similar classes of antibiotics, the antibiotic mecillinam (MEC) that inhibits PBP2 proteins was also examined [41]. BBH/MEC combination also demonstrates a synergistic effect with its FICI value of 0.5 (Table S3).

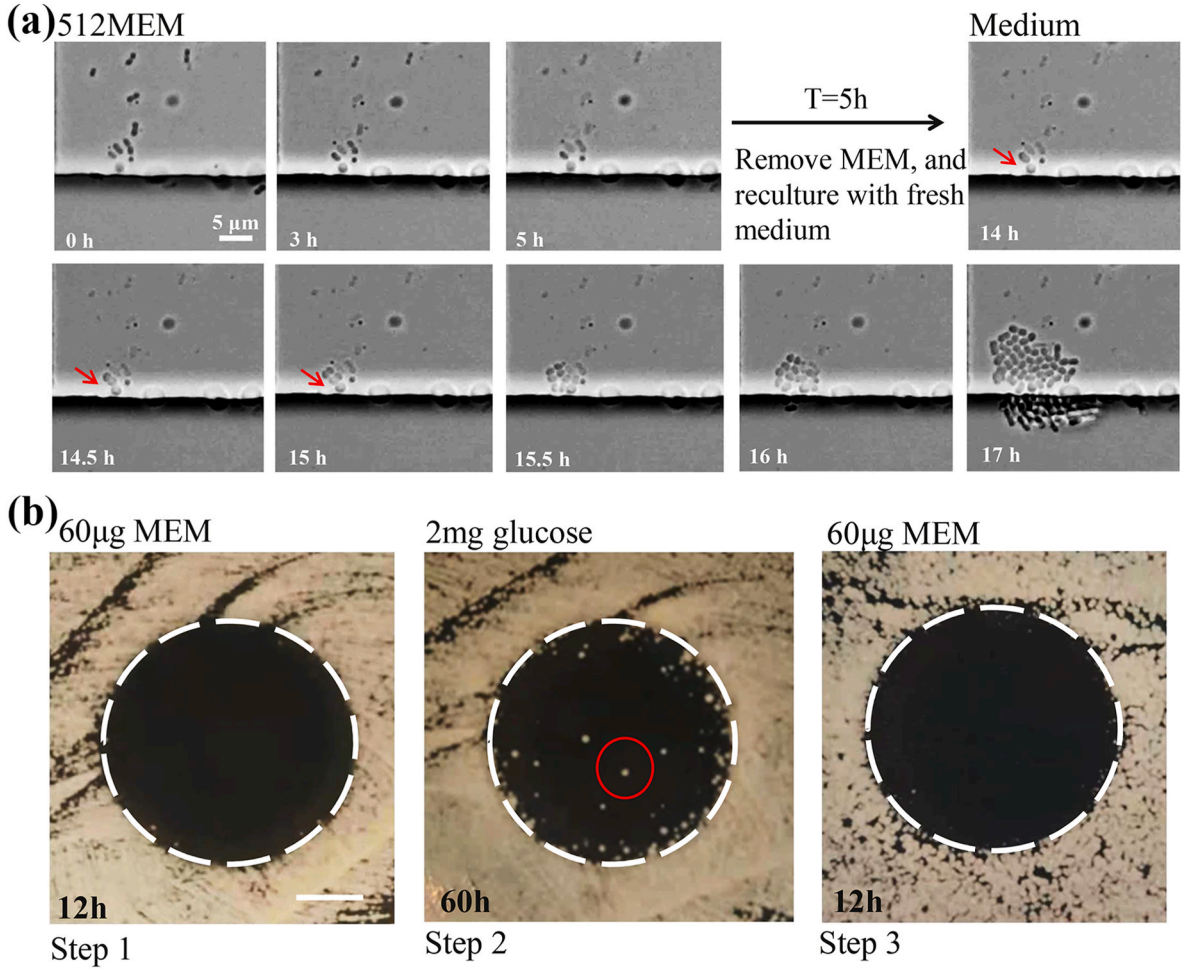

Fig. 3. (a) Bacterial persistence under a high dosage of MEM. After 5 h of treatment, the MEM solution was replaced with a fresh medium. No changes were observed in the first 9 h of culture in a fresh medium (data not shown). The red arrow indicates a persistent cell. (b) The TDtest essay. It was performed to verify bacterial tolerance or persistence under a high dosage of MEM treatment. Step 1: the diameter of the inhibition zone = 19 mm (indicated by an open white circle). Step 2: colonies indicated with a red circle formed inside the inhibition zone after glucose addition, indicating the tolerant/persistent cells. Step 3: The diameter of the inhibition zone (indicated by an open white circle) for the tolerant/persistent cells (originated from the single colony indicated with a red circle in Step 2) is 19 mm, the same as its parental strain. MEM: meropenem.

On-chip assay of the BBH/MEM and BBH/MEC combinations were carried out at their respective MIC values. At the BBH (256 mg/L)-MEM (16 mg/L) combination, many cells became swollen within 40 min. After 2 h, almost all cells were swollen to a certain degree and were stained as dead cells, indicating compromised membranes of bacteria (Fig. 4a). After 2 h of the treatment, the fresh medium was re-introduced to culture cells; however, no cells were found to resume growth (Fig. S4). This phenomenon was in drastic contrast with single MEM of 16 mg/L, where most of the cells kept dividing during the whole period of treatment, and only a few cells became swollen (Fig. 2b, red arrow indicated). This early transition to the swollen morphology was also observed at the MIC concentration of MEM alone (i.e., 64 mg/L) (Fig. 2b), indicating BBH may have contributed to the MEM accumulation within cells and consequently accelerated the killing process.

Similarly, when cells were treated with 256 mg/L of MEC alone, cells swelled, and continuous cell division was observed -similar to cell response at 16 mg/L of MEM (Fig. 4a). This phenotype between MEM and MEC is similar since both of them inhibit PBP2 proteins [41]. However, at the BBH (256 mg/L)-MEC (256 mg/L) combination, almost all cells remained unchanged throughout the whole treatment and were characterised as dead cells via live/dead staining (Fig. 4a) or re-culture method (Fig. S4). Cell growth rates were also reduced under treatment with either MEM/BBH or MEC/BBH (Fig. 4b). These results corroborate well with our recent finding that BBH is bound to the AdeB multi-drug transporter protein in *A. baumannii*, which could contribute to reduced extrusion of antibiotics by the AdeABC pump [30].

3.4. Kinetic studies of antibiotic combination on-chip

The kinetics of an antibiotic in the body (e.g., changes in antibiotic concentration) play a vital role in determining the success of treatments as well as minimizing the emergence of resistance [42–44]. For an antibiotic combination, each compound may have different pharmacokinetics, and not all the compounds can reach the targeted site at the same time. To understand whether this time interval between the compounds affects the killing efficiency of a combination, we carried out a series of kinetic studies, varying the different sequences and intervals of delivering MEM or BBH at the MIC concentration of the MEM/BBH combination.

Considering the doubling time of cells on-chip is ~26 min (Table S2), we treated cells first with either 16 mg/L BBH or 256 mg/L MEM for 40 min and followed by the BBH/MEM combination at its MIC value (denoted as 16 MEM (40min)-16 MEM/256 BBH (140min) or 256 BBH (40min)-16 MEM/256 BBH (140min)). Similar to the phenomena observed above (Fig. 4a), most cells were dividing within the first 40 min but became swollen at 80 min (Fig. 5), indicating the mechanism of action of BBH or MEM. Surprisingly, most cells became swollen and divided continuously under the subsequent treatment of BBH/MEM. This contrast with the effective killing observed when the combination drug was delivered together from the onset (Fig. 4a). However, when the interval between the sequential mono-treatment in the MEM/BBH combination was reduced to 10 min before substantial cell swelling occurred (denoted as 256 BBH (10min)-16 MEM/256 BBH (170min)), the killing efficiency of the combination was comparable to the 16 MEM/256 BBH treatment without interval (Fig. 5, Fig. S5).

To further examine the discoveries from the single-cell approach, similar evaluations were conducted with conventional bulk culture, where cells were treated with a single compound (either 256 mg/L BBH or 16 mg/L MEM) for a series of different durations firstly (i.e., 0.5h, 1h, 2h, 4h, and 6h) and followed by the BBH/MEM combination treatments. In both scenarios, the inhibition rates decreased with increased intervals compared to no pre-single combination treatment (i.e., MEM/BBH) (Fig. 6). The inhibition rates dropped below 90% in pre-treatments 1 h for 16 mg/L MEM and 4 h for 256 mg/L BBH. These results highlighted that the dynamic or time-course interaction between compounds could eliminate the synergistic effects of combination treatments and induce an adverse impact. Therefore, a thorough evaluation of their pharmacokinetic/pharmacodynamic (PK/PD) parameters is essential to realize their synergistic effects in tackling MDR-bacterial infection.

4. Discussion

In the era of increased bacterial resistance to existing antibiotics, whilst no new classes of antibiotics for Gram-negative pathogens are available in the near future, antibiotic combinations offer an important strategy to combat resistant strains (especially those on the WHO priority list) and prolong the lifetime of clinically validated drugs [8]. An ideal combination treatment can improve killing efficacy, suppresses the emergence of resistance and minimize toxicity to the host. In addition, drug combinations would normally be applied to severe infections

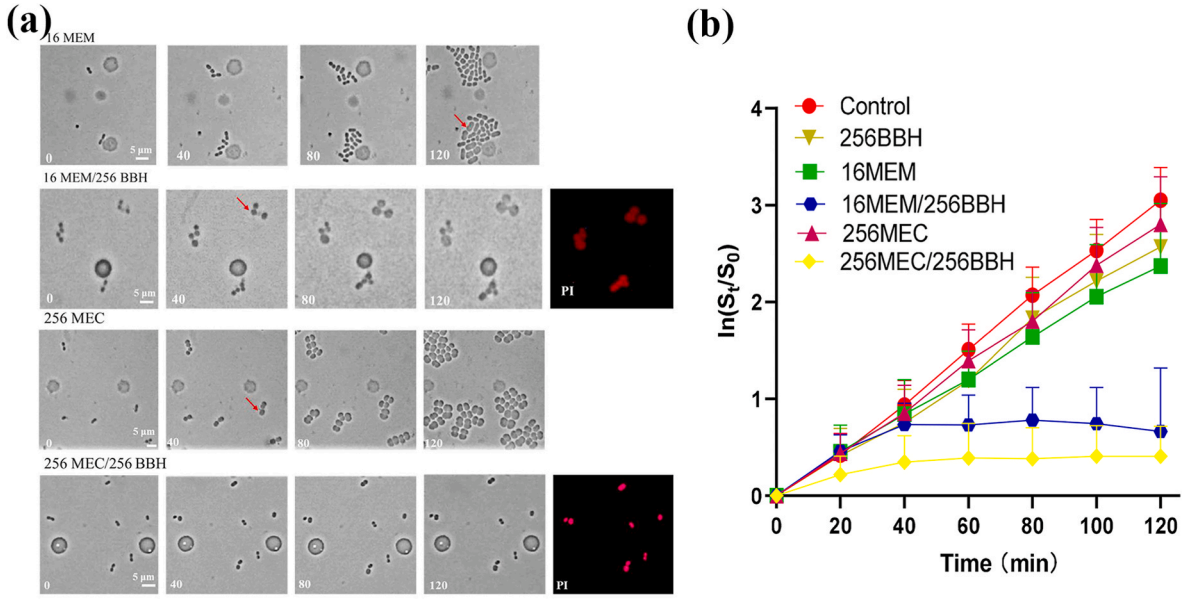

Fig. 4. (a) Time-lapse images of cells under single/combined drug treatments for 120 min. Dead cells in combinational treatments at the end of testing were stained with propidium iodide (PI), represented in red. (b) Correlated growth curves. BBH: berberine hydrochloride; MEM: meropenem; MEC: mecillinam.

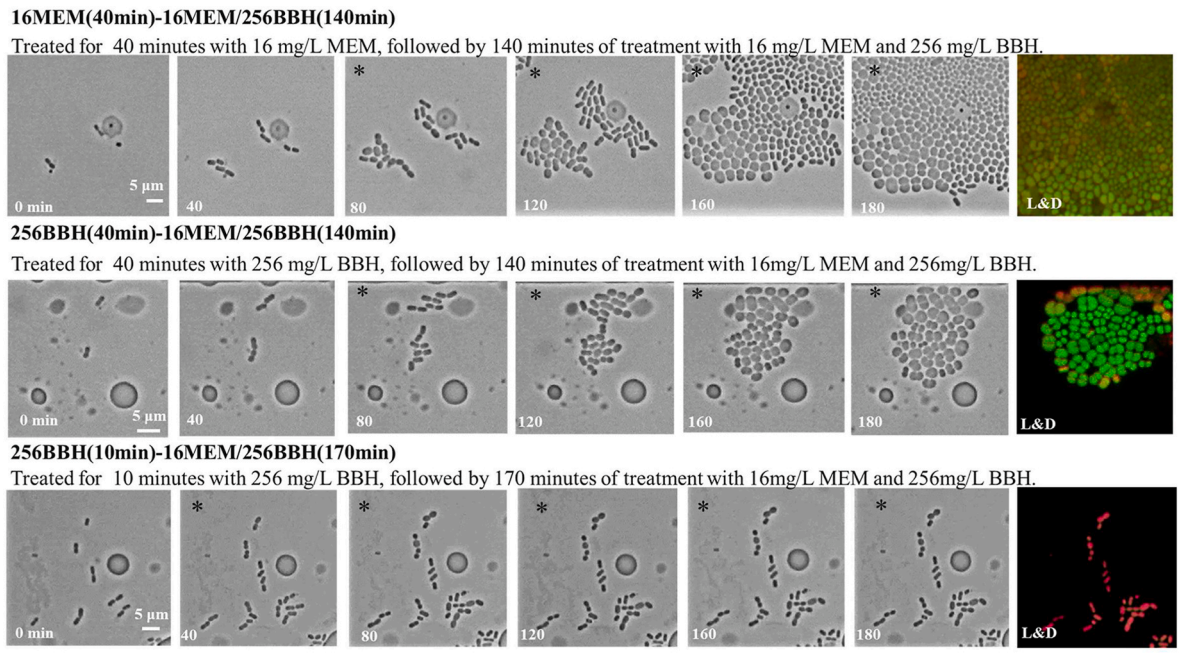

Fig. 5. Kinetic studies of MEM/BBH combinational treatments for 180 min. The period of cells under each treatment was indicated in the above images. "*" denoted the periods where bacteria were treated with the combination of MEM/BBH. Live/dead cell staining was performed at the end of the tests. BBH: berberine hydrochloride; MEM: meropenem.

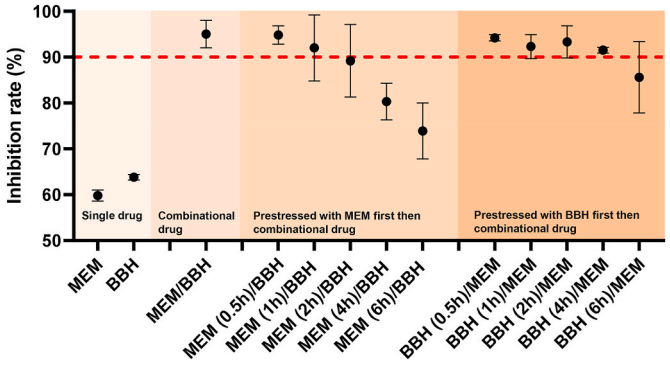

Fig. 6. BBH/MEM combination tests in 96-well plates. Drugs were added together or at different time intervals. Cells were treated with the first drug (the one before "/") for the period indicated in the brackets before the addition of the second drug. The total treatment period was fixed at 24 h. Inhibition rate = $[1-(OD_{600nm\ drugs\ +\ bacteria}-OD_{600nm\ medium})/(OD_{600nm\ medium\ +\ bacteria}-OD_{600nm\ medium})] \times 100\%$. The combinational treatments with inhibition rates above 90% (i.e., the red dotted line) were effective against bacteria. The concentration of MEM and BBH are 16 mg/L and 256 mg/L, respectively. BBH: berberine hydrochloride; MEM: meropenem.

where causative pathogens often feature multi-resistance and various survival modes (e.g., tolerance and heteroresistance) [9,45]. To date, the mechanism of action in most empirical antibiotic combinations used in clinical is poorly understood [8].

In the past decades, advances in single-cell analysis have significantly facilitated the discoveries of mechanisms underlying bacterial response to antibiotic stresses [45,46]. For instance, single-cell microfluidics platforms have been developed for rapid antibiotic susceptibility testing [47,48] and studying antibiotic resistance mechanisms [49]. However, there are limited studies to investigate the dynamics of combination drugs towards the same/historical bacteria in situ observation. With our single-cell microfluidic system, morphological changes of native cells were recorded in real-time. Since morphological transformation is part of bacteria's normal life cycle in response to stress (such as starvation, and antibiotics) [50], this provides rich information to study the mode of action and the resistance mechanisms under different drug treatments sequentially.

By obtaining the growth characteristics of individual cells, we revealed the heterogeneous response of MDR *A. baumannii* under different antibiotic treatments (Fig. 2b; Fig. 4a; Fig. 5). The ability of programmable delivery of multiple treatments on the same cells enabled us to track correlated (or historical) responses of individual cells, revealing unprecedented information to study mode of action. We found BBH alone had a weak inhibition effect on MDR *A. baumannii*, while high concentrations of MEM alone showed effective killing efficiency; the persistence cells also existed. Importantly, with the ability to dynamically exchange reagents, and remove and retrieve cells off-chip for long-term investigations, this platform allowed us to study the dynamic interaction of the compounds. To date, most in vitro evaluations of drug combinations are based on the endpoint and population measurements of defined formulations; however, such approaches fail to consider different kinetic factors of each compound in vivo (e.g., different pharmacodynamics). As we illustrated for the first time, the outcome of cells being treated with or without time intervals between the two compounds in a combination could be significantly different. For the BBH/MEM combination, the initial treatment (i.e., >1 doubling time) of the cells with any compound could eliminate the synergistic effect of the combination (Figs. 5 and 6). This discovery may illuminate many previous reports of discrepancies between in vitro and in vivo evaluations [51,52], highlighting the importance of evaluating pharmacodynamic interactions of drug combinations in vitro or in vivo using traditional methods or lab-on-a-chip-based approaches [53].

5. Conclusion

With the single-cell microfluidic approach, various mechanisms resisting antibiotic treatments have been discovered, including rare persistence cells triggered by high-dose antibiotic treatments. It has been found that the efficacy of synergistic combinations could be severely reduced if the bacteria were pre-treated by any of the compounds. The discoveries illustrate that understanding the potential

pharmacokinetics of antibiotic combinations is pivotal to predicting their clinical utility and reducing the emergence of new resistances. Overall, our platform provided unique dynamic information on bacteria under different drug treatments and in-depth kinetic analysis for combination treatment in vitro, which may aid in drug discovery or large-scale screening for synergistic combinations against MDR-bacterial infection.

Credit author statement

Xiaobo Li: Methodology, Formal analysis, Investigation, Writing - Original Draft, Writing - Review & Editing, Visualization. **Yanqing Song**: Methodology, Validation, Formal analysis, Investigation, Writing - Original Draft. **Xiuzhao Chen**: Validation, Formal analysis, Visualization. **Jianan Yin**: Validation, Formal analysis. **Ping Wang**: Conceptualization, Software, Resources, Supervision. **He Huang**: Conceptualization, Software, Resources, Writing - Original Draft, Supervision, Project administration, Funding acquisition. **Huabing Yin**: Conceptualization, Software, Resources, Writing - Original Draft, Writing - Review & Editing, Supervision, Project administration, Funding acquisition.

Declaration of competing interest

The authors declare that they have no known competing financial interests or personal relationships that could have appeared to influence the work reported in this paper.

Data availability

Data will be made available on request.

Acknowledgements

This work was supported by grants from National Key Research and Development Project (No. 2019YFA0905600), Science and Technology Program of Tianjin, China (No. 22YFZCSN00090). We thank the support of NERC (NE/S008721/1) and EPSRC IAA (EP/R511705/1).

Appendix A. Supplementary data

Supplementary data to this article can be found online at https://doi.org/10.1016/j.talanta.2023.124814.

References

[1] U. Theuretzbacher, K. Bush, S. Harbarth, M. Paul, J.H. Rex, E. Tacconelli, G. E. Thwaites, Critical analysis of antibacterial agents in clinical development, Nat. Rev. Microbiol. 18 (2020) 286–298, https://doi.org/10.1038/s41579-020-0340-0.
[2] U. Theuretzbacher, K. Outterson, A. Engel, A. Karlen, The global preclinical antibacterial pipeline, Nat. Rev. Microbiol. 18 (2020) 275–285, https://doi.org/10.1038/s41579-019-0288-0.
[3] J. Cama, R. Leszczynski, P.K. Tang, A. Khalid, V. Lok, C.G. Dowson, A. Ebata, To push or to pull? In a post-COVID world, supporting and incentivizing antimicrobial drug development must become a governmental priority, ACS Infect. Dis. 7 (2021) 2029–2042, https://doi.org/10.1021/acsinfecdis.0c00681.
[4] S. Mohd Sazlly Lim, A. Zainal Abidin, S.M. Liew, J.A. Roberts, F.B. Sime, The global prevalence of multidrug-resistance among Acinetobacter baumannii causing hospital-acquired and ventilator-associated pneumonia and its associated mortality: a systematic review and meta-analysis, J. Infect. 79 (2019) 593–600, https://doi.org/10.1016/j.jinf.2019.09.012.
[5] N. Cassir, J.M. Rolain, P. Brouqui, A new strategy to fight antimicrobial resistance: the revival of old antibiotics, Front. Microbiol. 5 (2014) 551, https://doi.org/10.3389/fmicb.2014.00551.
[6] M. Kempf, J.M. Rolain, Emergence of resistance to carbapenems in Acinetobacter baumannii in Europe: clinical impact and therapeutic options, Int. J. Antimicrob. Agents 39 (2012) 105–114, https://doi.org/10.1016/j.ijantimicag.2011.10.004.
[7] T. Tängdén, Combination antibiotic therapy for multidrug-resistant Gram-negative bacteria, Ups. J. Med. Sci. 119 (2014) 149–153, https://doi.org/10.3109/03009734.2014.899279.
[8] M. Tyers, G.D. Wright, Drug combinations: a strategy to extend the life of antibiotics in the 21 st century, Nat. Rev. Microbiol. 17 (2019) 141–155, https://doi.org/10.1038/s41579-018-0141-x.
[9] J.F. Liu, O. Gefen, I. Ronin, M. Bar-Meir, N.Q. Balaban, Effect of tolerance on the evolution of antibiotic resistance under drug combinations, Science 367 (2020) 200, https://doi.org/10.1126/science.aay3041.
[10] W.E. Rose, A.D. Berti, J.B. Hatch, D.G. Maki, Relationship of in vitro synergy and treatment outcome with daptomycin plus rifampin in patients with invasive methicillin-resistant Staphylococcus aureus infections, Antimicrob. Agents Chemother. 57 (2013) 3450–3452, https://doi.org/10.1128/AAC.00325-12.
[11] E.I. Nielsen, L.E. Friberg, Pharmacokinetic-pharmacodynamic modeling of antibacterial drugs, Pharmacol. Rev. 65 (2013) 1053–1090, https://doi.org/10.1124/pr.111.005769.
[12] M.A. Sanchez-Romero, J. Casadesus, Contribution of phenotypic heterogeneity to adaptive antibiotic resistance, Proc. Natl. Acad. Sci. U.S.A. 111 (2014) 355–360, https://doi.org/10.1073/pnas.1316084111.
[13] I. Levin-Reisman, I. Ronin, O. Gefen, I. Braniss, N. Shoresh, N.Q. Balaban, Antibiotic tolerance facilitates the evolution of resistance, Science 355 (2017) 826–830, https://doi.org/10.1126/science.aaj2191.
[14] N.Q. Balaban, S. Helaine, K. Lewis, M. Ackermann, B. Aldridge, D.I. Andersson, M. P. Brynildsen, D. Bumann, A. Camilli, J.J. Collins, C. Dehio, S. Fortune, J.M. Ghigo, W.D. Hardt, A. Harms, M. Heinemann, D.T. Hung, U. Jenal, B.R. Levin, J. Michiels, G. Storz, M.W. Tan, T. Tenson, L. Van Melderen, A. Zinkernagel, Definitions and guidelines for research on antibiotic persistence, Nat. Rev. Microbiol. 17 (2019) 441–448, https://doi.org/10.1038/s41579-019-0196-3.
[15] M. Ayrapetyan, T.C. Williams, R. Baxter, J.D. Oliver, Viable but nonculturable and persister cells coexist stochastically and are induced by human serum, Infect. Immun. 83 (2015) 4194–4203, https://doi.org/10.1128/IAI.00404-15.
[16] Y. Kaplan, S. Reich, E. Oster, S. Maoz, I. Levin-Reisman, I. Ronin, O. Gefen, O. Agam, N.Q. Balaban, Observation of universal ageing dynamics in antibiotic persistence, Nature 600 (2021) 290–294, https://doi.org/10.1038/s41586-021-04114-w.
[17] I. Levin-Reisman, A. Brauner, I. Ronin, N.Q. Balaban, Epistasis between antibiotic tolerance, persistence, and resistance mutations, Proc. Natl. Acad. Sci. U.S.A. 116 (2019) 14734–14739, https://doi.org/10.1073/pnas.1906169116.
[18] E.M. Windels, J.E. Michiels, B. Van den Bergh, M. Fauvart, J. Michiels, Antibiotics: combatting tolerance to stop resistance, mBio 10 (2019), e02095, https://doi.org/10.1128/mBio.02095-19, 19.
[19] R. Xie, A. Korolj, C. Liu, X. Song, R.X.Z. Lu, B. Zhang, A. Ramachandran, Q. Liang, M. Radisic, H-FIBER: microfluidic topographical hollow fiber for studies of glomerular filtration barrier, ACS Cent. Sci. 6 (6) (2020) 903–912, https://doi.org/10.1021/acscentsci.9b01097.
[20] R. Xie, Z. Liang, Y. Ai, W. Zheng, J. Xiong, P. Xu, Y. Liu, M. Ding, J. Gao, J. Wang, Q. Liang, Composable microfluidic spinning platforms for facile production of biomimetic perfusable hydrogel microtubes, Nat. Protoc. 16 (2) (2021) 937–964, https://doi.org/10.1038/s41596-020-00442-9.
[21] B. Li, Y. Qiu, J. Zhang, X. Huang, H.C. Shi, H.B. Yin, Real-time study of rapid spread of antibiotic resistance plasmid in biofilm using microfluidics, Environ. Sci. Technol. 52 (2018) 11132–11141, https://doi.org/10.1021/acs.est.8b03281.
[22] J.M. Nathalie Q. Balaban, Remy Chait, Lukasz Kowalik, Stanislas Leibler, Bacterial persistence as a phenotypic switch, Science 305 (2004) 1622–1625, https://doi.org/10.1126/science.1099390.
[23] B. Li, Y. Qiu, A. Glidle, D. Mcilvenna, Q. Luo, J. Cooper, H.-C. Shi, H. Yin, Gradient microfluidics enables rapid bacterial growth inhibition testing, Anal. Chem. 86 (2014) 3131–3137, https://doi.org/10.1021/ac5001306.
[24] Y. Ai, R. Xie, J. Xiong, Q. Liang, Microfluidics for biosynthesizing: from droplets and vesicles to artificial cells, Small 16 (9) (2020), 1903940, https://doi.org/10.1002/smll.201903940.
[25] O. Goode, A. Smith, A. Zarkan, J. Cama, B.M. Invergo, D. Belgami, S. Caño-Muñiz, J. Metz, P. O'Neill, A. Jeffries, I.H. Norville, J. David, D. Summers, S. Pagliara, Persister Escherichia coli cells have a lower intracellular pH than susceptible cells but maintain their pH in response to antibiotic treatment, mBio 12 (2021), e00909-e00921, https://doi.org/10.1128/mBio.00909-21.
[26] J. Choi, J. Yoo, M. Lee, E.G. Kim, J.S. Lee, S. Lee, S. Joo, S.H. Song, E.C. Kim, J. C. Lee, H.C. Kim, Y.G. Jung, S. Kwon, A rapid antimicrobial susceptibility test based on single-cell morphological analysis, Sci. Transl. Med. 6 (2014) 13, https://doi.org/10.1126/scitranslmed.3009650.
[27] B. Li, Y. Qiu, Y. Song, H. Lin, H. Yin, Dissecting horizontal and vertical gene transfer of antibiotic resistance plasmid in bacterial community using microfluidics, Environ. Int. 131 (2019), 105007, https://doi.org/10.1016/j.envint.2019.105007.
[28] B. Li, Y. Qiu, A. Glidle, J. Cooper, H. Shi, H. Yin, Single cell growth rate and morphological dynamics revealing an "opportunistic" persistence, Analyst 139 (2014) 3305–3313, https://doi.org/10.1039/c4an00170b.
[29] D.I. Andersson, N.Q. Balaban, F. Baquero, P. Courvalin, P. Glaser, U. Gophna, R. Kishony, S. Molin, T. Tonjum, Antibiotic resistance: turning evolutionary principles into clinical reality, FEMS Microbiol. Rev. 44 (2020) 171–188, https://doi.org/10.1093/femsre/fuaa001.
[30] X. Li, Y. Song, L. Wang, G. Kang, P. Wang, H. Yin, H. Huang, A potential combination therapy of berberine hydrochloride with antibiotics against multidrug-resistant acinetobacter baumannii, Front. Cell. Infect. Microbiol. 11 (2021), 660431, https://doi.org/10.3389/fcimb.2021.660431.
[31] X. Yuan, J.M. Couto, A. Glidle, Y. Song, W. Sloan, H. Yin, Single-cell microfluidics to study the effects of genome deletion on bacterial growth behavior, ACS Synth. Biol. 6 (2017) 2219–2227, https://doi.org/10.1021/acssynbio.7b00177.

[32] H. Huang, Z.L. Yang, X.M. Wu, Y. Wang, Y.J. Liu, H. Luo, X. Lv, Y.R. Gan, S. D. Song, F. Gao, Complete genome sequence of Acinetobacter baumannii MDR-TJ and insights into its mechanism of antibiotic resistance, J. Antimicrob. Chemother. 67 (2012) 2825–2832, https://doi.org/10.1093/jac/dks327.
[33] Clinical, Performance Standards for Antimicrobial Susceptibility Testing. Twenty-Eighth Informational Supplement. Document M100. CLSI, Clinical and Laboratory Standards Institute, Wayne, PA, 2018.
[34] L.K. Caesar, N.B. Cech, Synergy and antagonism in natural product extracts: when 1 + 1 does not equal 2, Nat. Prod. Rep. 36 (2019) 869–888, https://doi.org/10.1039/c9np00011a.
[35] O. Gefen, B. Chekol, J. Strahilevitz, N.Q. Balaban, TDtest: easy detection of bacterial tolerance and persistence in clinical isolates by a modified disk-diffusion assay, Sci. Rep. 7 (2017), 41284, https://doi.org/10.1038/srep41284.
[36] O. Fridman, A. Goldberg, I. Ronin, N. Shoresh, N.Q. Balaban, Optimization of lag time underlies antibiotic tolerance in evolved bacterial populations, Nature 513 (2014) 418–421, https://doi.org/10.1038/nature13469.
[37] B. Li, Y. Qiu, H. Shi, H. Yin, The importance of lag time extension in determining bacterial resistance to antibiotics, Analyst 141 (2016) 3059–3067, https://doi.org/10.1039/c5an02649k.
[38] P. Macheboeuf, C. Contreras-Martel, V. Job, O. Dideberg, A. Dessen, Penicillin binding proteins: key players in bacterial cell cycle and drug resistance processes, FEMS Microbiol. Rev. 30 (2006) 673–691, https://doi.org/10.1111/j.1574-6976.2006.00024.x.
[39] R.A. Fisher, B. Gollan, S. Helaine, Persistent bacterial infections and persister cells, Nat. Rev. Microbiol. 15 (2017) 453–464, https://doi.org/10.1038/nrmicro.2017.42.
[40] M. Huemer, S. Mairpady Shambat, S.D. Brugger, A.S. Zinkernagel, Antibiotic resistance and persistence—implications for human health and treatment perspectives, EMBO Rep. 21 (2020), e51034, https://doi.org/10.15252/embr.202051034.
[41] W.F. Penwell, A.B. Shapiro, R.A. Giacobbe, R.F. Gu, N. Gao, J. Thresher, R. E. McLaughlin, M.D. Huband, B.L. DeJonge, D.E. Ehmann, A.A. Miller, Molecular mechanisms of sulbactam antibacterial activity and resistance determinants in Acinetobacter baumannii, Antimicrob. Agents Chemother. 59 (2015) 1680–1689, https://doi.org/10.1128/AAC.04808-14.
[42] M.E. Falagas, K.Z. Vardakas, K.P. Tsiveriotis, N.A. Triarides, G.S. Tansarli, Effectiveness and safety of high-dose tigecycline-containing regimens for the treatment of severe bacterial infections, Int. J. Antimicrob. Agents 44 (2014) 1–7, https://doi.org/10.1016/j.ijantimicag.2014.01.006.
[43] M. Sabet, Z. Tarazi, D.C. Griffith, Pharmacodynamics of meropenem against acinetobacter baumannii in a neutropenic mouse thigh infection model, Antimicrob. Agents Chemother. 64 (2020), e02388, https://doi.org/10.1128/AAC.02388-19, 19.
[44] N. Kumta, A.J. Heffernan, M.O. Cotta, S.C. Wallis, A. Livermore, T. Starr, W. T. Wong, G.M. Joynt, J. Lipman, J.A. Roberts, Plasma and cerebrospinal fluid population pharmacokinetics of meropenem in neurocritical care patients: a prospective two-center study, Antimicrob. Agents Chemother. 66 (2022), e00142, https://doi.org/10.1128/aac.00142-22, 22.
[45] I. Levin-Reisman, A. Brauner, I. Ronin, N.Q. Balaban, Epistasis between antibiotic tolerance, persistence, and resistance mutations, Proc. Natl. Acad. Sci. U.S.A. 116 (2019) 14734–14739, https://doi.org/10.1073/pnas.1906169116.
[46] S. Nolivos, J. Cayron, A. Dedieu, A. Page, F. Delolme, C. Lesterlin, Role of AcrAB-TolC multidrug efflux pump in drug-resistance acquisition by plasmid transfer, Science 364 (2019) 778–782, https://doi.org/10.1126/science.aav6390.
[47] N. Qin, P. Zhao, E.A. Ho, G. Xin, C.L. Ren, Microfluidic technology for antibacterial resistance study and antibiotic susceptibility testing: review and perspective, ACS Sens. 6 (1) (2021) 3–21.
[48] S. Hwang, J. Choi, Rapid antimicrobial susceptibility testing for low bacterial concentrations integrating a centrifuge based bacterial cell concentrator, Lab Chip 23 (2) (2023) 229–238.
[49] Y. Zhang, I. Kepiro, M.G. Ryadnov, S. Pagliara, Single cell killing kinetics differentiate phenotypic bacterial responses to different antibacterial classes, Microbiol. Spectr. 11 (1) (2023), e03667, 22.
[50] D.L. Popham, K.D. Young, Role of penicillin-binding proteins in bacterial cell morphogenesis, Curr. Opin. Microbiol. 6 (2003) 594–599, https://doi.org/10.1016/j.mib.2003.10.002.
[51] M. Paul, G.L. Daikos, E. Durante-Mangoni, D. Yahav, Y. Carmeli, Y.D. Benattar, A. Skiada, R. Andini, N. Eliakim-Raz, A. Nutman, O. Zusman, A. Antoniadou, P. C. Pafundi, A. Adler, Y. Dickstein, I. Pavleas, R. Zampino, V. Daitch, R. Bitterman, H. Zayyad, F. Koppel, I. Levi, T. Babich, L.E. Friberg, J.W. Mouton, U. Theuretzbacher, L. Leibovici, Colistin alone versus colistin plus meropenem for treatment of severe infections caused by carbapenem-resistant Gram-negative bacteria: an open-label, randomised controlled trial, Lancet Infect. Dis. 18 (2018) 391–400, https://doi.org/10.1016/S1473-3099(18)30099-9.
[52] W. Katip, S. Uitrakul, P. Oberdorfer, A comparison of colistin versus colistin plus meropenem for the treatment of carbapenem-resistant acinetobacter baumannii in critically ill patients: a propensity score-matched analysis, Antibiotics (Basel) 9 (10) (2020) 647, https://doi.org/10.3390/antibiotics9100647.
[53] Y. Ai, F. Zhang, C. Wang, R. Xie, Q. Liang, Recent progress in lab-on-a-chip for pharmaceutical analysis and pharmacological/toxicological test, TrAC, Trends Anal. Chem. 117 (2019) 215–230, https://doi.org/10.1016/j.jpba.2021.114534.